Available online at www.sciencedirect.com
ScienceDirect
Trans. Nonferrous Met. Soc. China 22(2012) 262−267
Transactions of Nonferrous Metals Society of China
www.tnmsc.cn

Structure stability and mechanical properties of high-pressure die-cast Mg−Al−Ce−Y-based alloy

ZHANG Jing-huai[1], LIU Shu-juan[2], LENG Zhe[1], ZHANG Mi-lin[1], MENG Jian[3], WU Rui-zhi[1]

1. Key Laboratory of Superlight Materials & Surface Technology of Ministry of Education, Harbin Engineering University, Harbin 150001, China;
2. School of Materials Science and Engineering, Harbin Institute of Technology, Harbin 150001, China;
3. State Key Laboratory of Rare Earth Resources Utilization, Changchun Institute of Applied Chemistry, Chinese Academy of Sciences, Changchun 130022, China

Received 28 February 2011; accepted 23 June 2011

Abstract: With the aim to further improve the mechanical properties of Mg−Al−RE-based alloy, Mg−3.0Al−1.8Ce−0.3Y−0.2Mn alloy was prepared by high-pressure die-casting technique. The microstructure, thermal stability of intermetallic phases and mechanical properties were investigated. The results show that the alloy is composed of fine primary α-Mg dendrites and eutectic in the interdendritic regions. The intermetallic phases in eutectic are $Al_{11}(Ce,Y)_3$ and $Al_2(Ce,Y)$ with the former being the dominant one. The thermal stability of $Al_{11}(Ce,Y)_3$ is conditioned. It is basically stable at temperature up to 200 °C within 800 h, while most of the $Al_{11}(Ce,Y)_3$ intermetallics transform to $Al_2(Ce,Y)$ at higher temperature of 450 °C for 800 h. The alloy exhibits remarkably improved strength both at room temperature and 200 °C, which is mainly attributed to the reinforcement of dendrite boundaries with $Al_{11}(Ce,Y)_3$ intermetallics, small dendritic arm spacing effect as well as the solid solution strengthening with Y element.
Key words: magnesium alloy; Mg−Al−Ce−Y alloy; $Al_{11}RE_3$; structure stability; mechanical properties

1 Introduction

In recent years, magnesium alloy in the form of high-pressure die-cast (HPDC) components has attracted much attention in automotive applications as advanced light material. Mg−Al-based alloys such as AZ91D and AM60B are used extensively in some non-critical parts [1]. However, these alloys are unsuitable for more critical components such as transmission and engine parts because of their poor mechanical properties at temperature above 125 °C [2, 3]. Further studies show that it is ascribed to the coarsening of β-$Mg_{17}Al_{12}$ phase in the eutectic region [4] and the discontinuous precipitate of lamellar $Mg_{17}Al_{12}$ from α-Mg matrix [5]. Moreover, a widely accepted view is that both diffusion controlled dislocation climbing and grain boundary sliding are the creep mechanisms in Mg−Al-based alloys [6]. Therefore, the design of alloys with good heat resistance should be based on the reinforcement of both the grain/dendrite boundaries and the α-Mg matrix.

The Mg−Al−RE series alloys such as AE42 are the typical heat-resistant alloys designed for lightweight applications in the automotive industry [7]. However, there still appear inconsistencies in the previous reports as to the stability of the main strengthening phase $Al_{11}RE_3$ in Mg−Al−RE alloys. PETTERSON et al [8] (AE42 heat treated at 150, 200 and 250 °C for 100 h), HUANG et al [9] (AE42, 450 °C for 15 h), ZHU et al [5] (AE42, 200 °C for 2 weeks), DARGUSCH et al [10] (AE42+1%Sr, 200 °C for 2 weeks) and RZYCHOŃ et al [11] (AE44, 175 °C for 3000 h) reported that the intermetallic phase $Al_{11}RE_3$ has high thermal stability, and no decomposition is observed. In contrast, according to the work by POWELL et al [12] (AE42, 175 °C for 1000 h with and without stress) and our recent work [13] (AE44, 200 °C for 100 h under 70 MPa stress), $Al_{11}RE_3$ is unstable and partially decomposes to Al_2RE.

Foundation item: Project (HEUCFR1128) supported by the Fundamental Research Funds for the Central Universities, China; Project (2010AA4BE031) supported by the Key Project of Science and Technology of Harbin City, China; Projects (20100471015, 20100471046) supported by the China Postdoctoral Science Foundation; Project (LBH-Z09217) supported by the Heilongjiang Postdoctorial Fund, China
Corresponding author: ZHANG Jing-huai; Tel: +86-451-82533026; E-mail: jinghuaizhang@gmail.com
DOI: 10.1016/S1003-6326(11)61169-2

In this work, a new heat-resistant HPDC Mg alloy was designed. Relatively low Al content was used to improve the die castability, form high melting point intermetallics and try to avoid the formation of $Mg_{17}Al_{12}$. Ce with low solid solubility in Mg (0.74%, mass fraction) was added to form large amount of Al−Ce intermetallic particles to reinforce the grain/dendrite boundaries [14]; Y with high solubility in Mg (12.4%, mass fraction) was expected to strengthen the α-Mg matrix [14]. The microstructure, thermal stability of intermetallic and mechanical properties at room temperature and 200 °C of HPDC Mg−Al−Ce−Y-based alloy were investigated.

2 Experimental

The chemical composition of the experimental alloy was Mg−3.0Al−1.8Ce−0.3Y−0.2Mn (ACY320). The reference alloy prepared under the same condition was Mg−3.3Al−0.2Mn (AM30). Commercial pure Mg and Al were used. Ce, Y and Mn were added in the form of Mg−20%Ce, Mg−20%Y and Al−10%Mn master alloys (mass fraction). Specimens were die cast using a 280 t clamping force cold chamber die-cast machine. About 20 kg raw materials were melted in a mild steel crucible. Pure argon was used as protective gas and refined gas. The molten metal was hand-ladled into the casting machine and the melt temperature prior to casting was about 700 °C. The die was equipped with an oil heating/cooling system and the temperature of the oil heater was set to 220 °C. The chemical compositions of the castings were determined by inductively coupled plasma atomic emission spectrometer.

The tensile samples were 70 mm in gauge length and 6 mm in gauge diameter, as shown in Fig. 1. Tensile tests were performed using Instron 5869 tensile testing machine at a strain rate of 1.1×10^{-3} s^{-1}. The experimental result in the study was the average value of at least four measured specimens. Metallographic sample was cut from the middle segment of the tensile bar. The microstructures and intermetallic phases were characterized by scanning electron microscope (SEM) equipped with an energy dispersive X-ray spectrometer (EDS) and X-ray diffractometer (XRD).

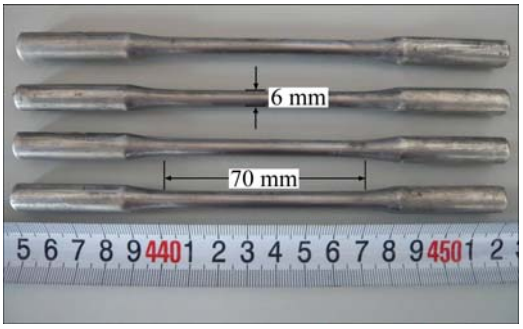

Fig. 1 Photo of HPDC tensile test bars obtained from ACY320 alloy

3 Results and discussion

3.1 Microstructure

In order to understand the role of Ce and Y additions in the Mg−3Al-based alloy, the microstructure of HPDC AM30 alloy is observed, as shown in Fig. 2(a). It reveals that the AM30 alloy is composed of primary α-Mg dendrites surrounded by interdendritic eutectic. A spot of β-$Mg1_7Al_{12}$ intermetallics disperses in the interdendritic regions. The average dendritic arm spacing (DAS) is about 17 μm. The remarkable changes in the microstructure can be observed with the addition of Ce and Y, as shown in Fig. 2(b). The primary α-Mg dendrites in HPDC ACY320 alloy tend to be equiaxed and the average DAS is reduced to 9 μm. More important, the amount of intermetallic compounds in the interdendritic regions is much higher than that in AM30 alloy with the similar Al content.

3.2 Intermetallics and their thermal stability

The XRD result of the HPDC ACY320 alloy is illustrated in Fig. 3(a). It is known that Mg−Al−Zn (AZ) and Mg−Al−Mn (AM) alloys are mainly composed of α-Mg and β-$Mg_{17}Al_{12}$ phases [15], the diffraction peaks of β-$Mg_{17}Al_{12}$ are not emerged due to the addition of Ce and Y. The main secondary phases in ACY320 alloy are $Al_{11}(Ce,Y)_3$ and $Al_2(Ce,Y)$, while the diffraction peak of $Al_{11}(Ce,Y)_3$ is much more intense than that of $Al_2(Ce,Y)$, which suggests that the former is the dominant one.

The magnified SEM images characterizing the secondary phases are shown in Figs. 2(c) and (d). The acicular intermetallics with length of 1−3 μm arrange in a row then the rows form layers roughly, which exhibits outstanding morphology and distribution of the intermetallics. Besides, a few polyhedral intermetallics with size of 1−5 μm can be observed by SEM observations. EDS analyses were used to identify these intermetallics. Figures 2(e) and (f) show the EDS spectra detected from acicular intermetallics and polyhedral intermetallic, respectively. Combined with the XRD result, the acicular intermetallic is identified as $Al_{11}(Ce,Y)_3$ and the polyhedral one corresponds to $Al_2(Ce,Y)$. It is worthwhile to note that $Al_{11}(Ce,Y)_3$ has higher content of Ce than Y, while Y content is much higher than Ce in $Al_2(Ce,Y)$.

To study the thermal stability of $Al_{11}(Ce,Y)_3$ intermetallic, some samples were aged at 200 and 450 °C for 800 h, respectively. The microstructure of ACY320 alloy after heat treatment is shown in Fig. 4. There is no obvious evidence of decomposition of the intermetallics in 200 °C annealed sample, except that a few particles

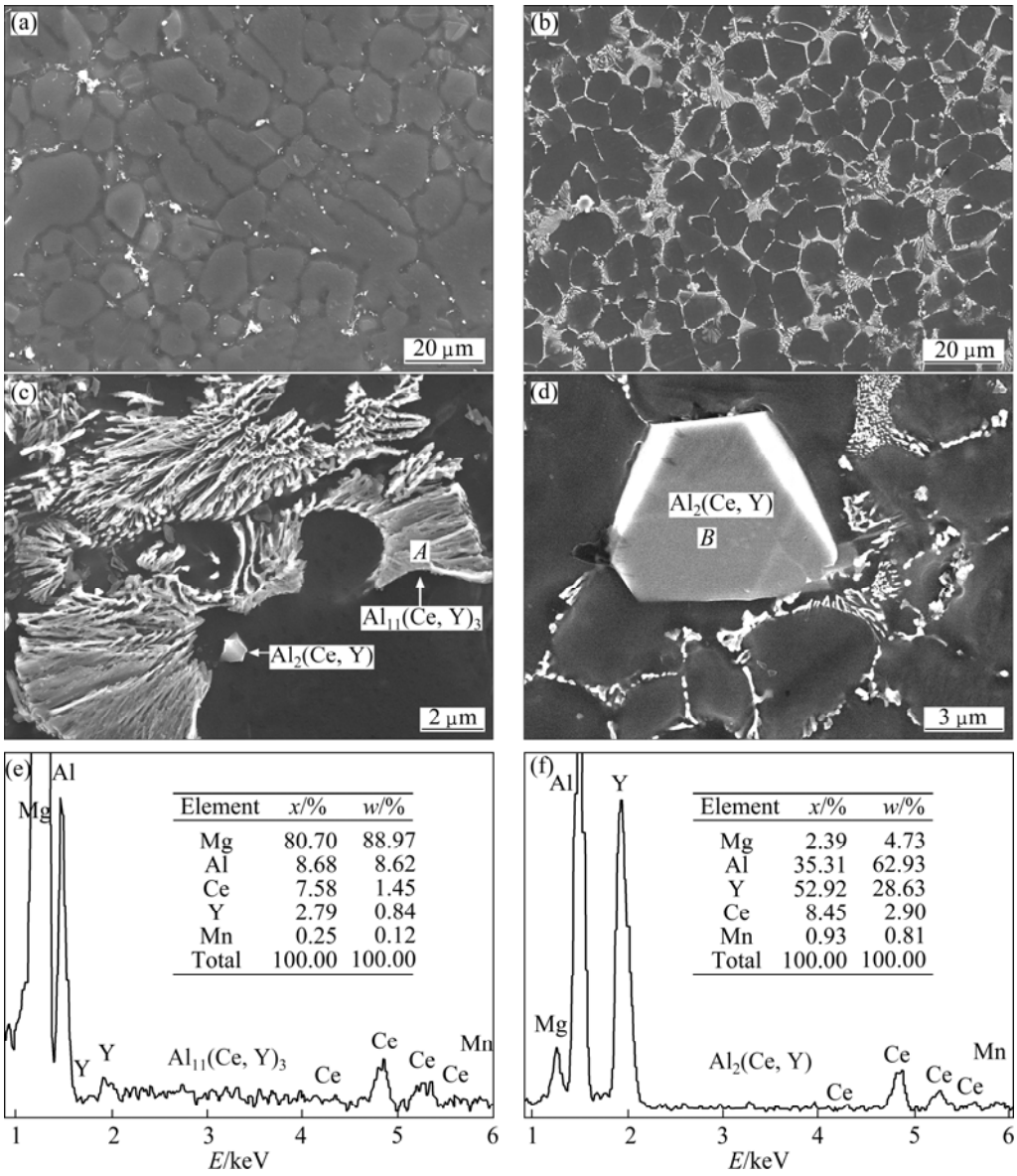

Element	x/%	w/%
Mg	80.70	88.97
Al	8.68	8.62
Ce	7.58	1.45
Y	2.79	0.84
Mn	0.25	0.12
Total	100.00	100.00

Element	x/%	w/%
Mg	2.39	4.73
Al	35.31	62.93
Y	52.92	28.63
Ce	8.45	2.90
Mn	0.93	0.81
Total	100.00	100.00

Fig. 2 SEM images and EDS analyses of HPDC alloys: (a) SEM images of AM30 alloy; (b, c, d) SEM images of HPDC ACY320 alloy; (e) EDS analyses of acicular intermetallics at point *A*; (f) EDS analyses of polyhedral intermetallic at point *B*

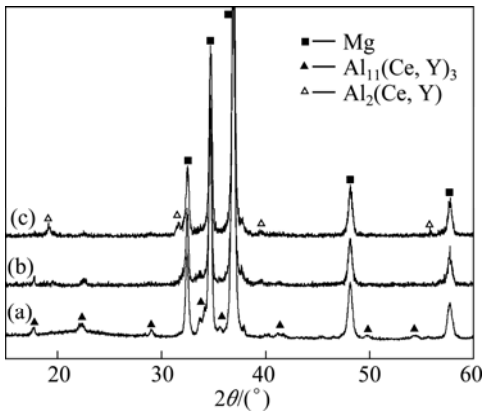

Fig. 3 XRD patterns of HPDC ACY320 alloys before aging (a), after aging at 200 °C for 800 h (b) and after aging at 450 °C for 800 h (c)

show certain coarsening (see Figs. 4(a)−(c)). The XRD patterns also show incognizable changes before and after 200 °C aging by comparing Figs. 3(a) and (b). However, the conspicuous change of microstructure could be observed after age treatment at higher temperature of 450 °C (Figs. 4(d)−(f)). It reveals that most of the acicular intermetallics disappear and give place to fine quadrate-like particles with size of 100−400 nm in interdendritic regions. The XRD pattern illustrated in Fig. 3(c) also changes obviously after 450 °C aging, namely, the intensity of $Al_{11}(Ce,Y)_3$ peaks decreases and that of $Al_2(Ce,Y)$ peaks increases obviously. In addition, EDS in SEM mode also indicates the Al: (Ce,Y) atom ratio of these small particles is close to 2:1, not 11:3. Therefore, the present study shows a clear evidence of

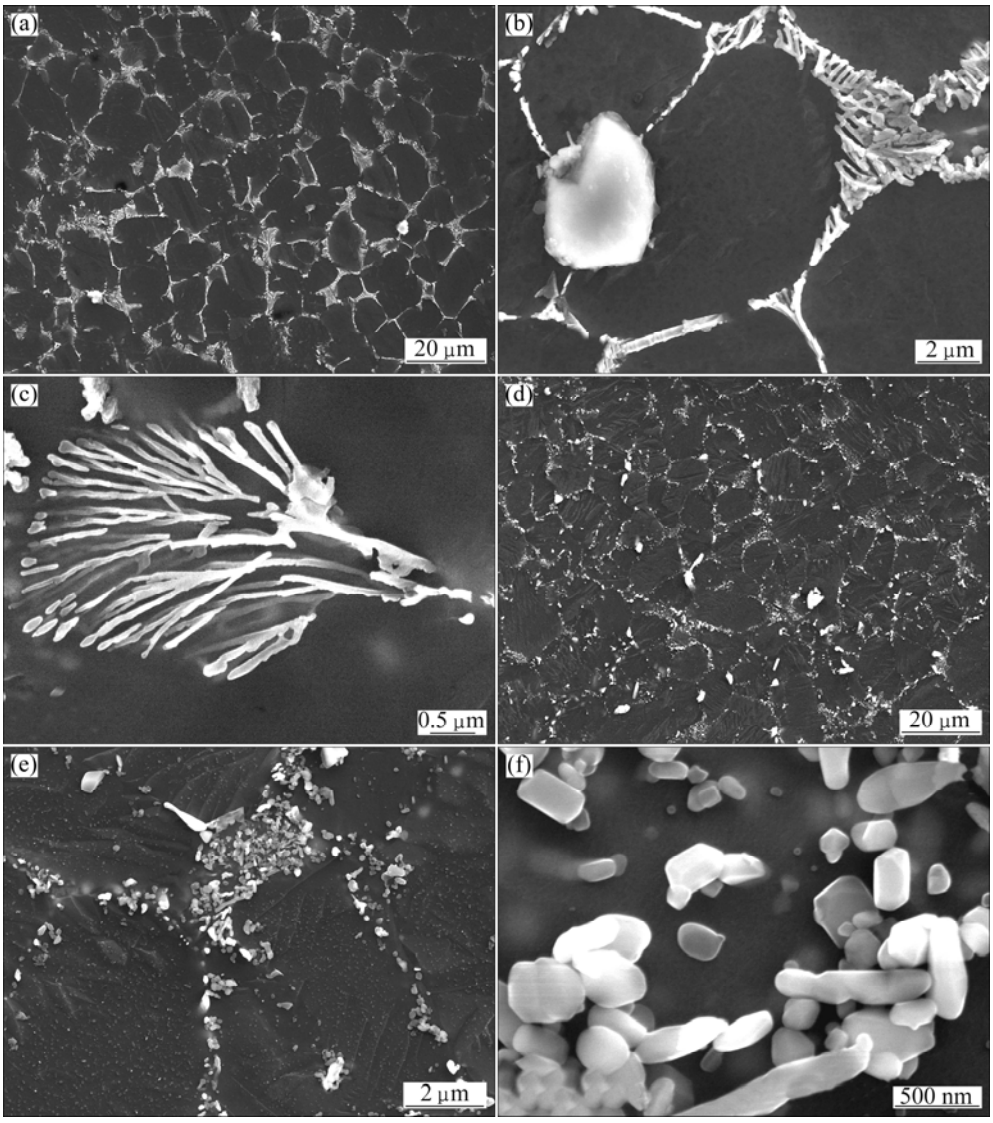

Fig. 4 SEM images of HPDC ACY320 after ageing at 200 °C (a, b, c) and 450 °C for 800 h (d, e, f)

the phase transition according to the reaction $Al_{11}(Ce,Y)_3 \longrightarrow 3Al_2(Ce, Y) + 5Al$ [12].

The observations reported here suggest that there is a limit to the thermal stability of $Al_{11}RE_3$. Up to now, the thermal stability of the main strengthening phase $Al_{11}RE_3$ in Mg−Al−RE alloys is still a matter of debate [6, 9−14]. POWELL et al [12] investigated the microstructural stability of die-cast AE42 (Mg−4Al−2RE) alloys which were individually creep tested for 1000 h at 22, 100, 125, 150 and 175 °C. It was reported that the lamellar/acicular phase $Al_{11}RE_3$, which dominates the interdendritic microstructure of the alloy, partly decomposes into Al_2RE and Al (forming $Mg_{17}Al_{12}$) at temperature above 150 °C (i.e. 175 °C), and the sharp decrease in the creep resistance is attributed to the reduced presence of the lamellar/acicular $Al_{11}RE_3$ and the appearance of $Mg_{17}Al_{12}$. In addition, it was also pointed out that the stress is not a contributing factor to $Al_{11}RE_3$ stability. However, ZHU et al [5] reported that intermetallic phase $Al_{11}RE_3$ in die-cast AE42 has high thermal stability with no decomposition observed at temperature up to 200 °C for 336 h, meanwhile, the continuous precipitation of $Mg_{17}Al_{12}$ due to the supersaturation of Al solute was observed in the Mg matrix, which was considered to be responsible for the deterioration in creep resistance at temperatures above 150 °C. In the present work, as for the alloy Mg−3.0Al−1.8Ce−0.3Y−0.2Mn after severe aging treatment at 200 °C for 800 h, neither obvious decomposition of $Al_{11}RE_3$ (i.e. $Al_{11}(Ce,Y)_3$) nor the formation of $Mg_{17}Al_{12}$ is observed. It is considered that following aspects are related to the stability of $Al_{11}RE_3$ and the formation of $Mg_{17}Al_{12}$. First, the harsh degree of aging treatment containing aging temperature and time is an important factor for the composition of $Al_{11}RE_3$. This may be responsible for the different observation results by POWELL et al (175 °C for 1000 h) and ZHU et al (200 °C for 336 h) in AE42 alloy as well as ACY320 alloy in this study (200 °C for 800 h and 450 °C for

800 h) at different aging temperatures. Second, the difference of RE components also affects the stability of $Al_{11}RE_3$ [13], which is a factor to explain the difference between $Al_{11}RE_3$ in AE42 and $Al_{11}(Ce, Y)_3$ in ACY320 alloy. Last, the lower Al content in ACY320 (3%) compared with that in AE42 (4%) causes little Al sequestered as soluted in the Mg matrix, which is responsible for no discernible precipitation of $Mg_{17}Al_{12}$ after aging in ACY320 alloy. The absence of DSC analysis to study phase transition challenges further work.

3.3 Mechanical properties

The representative tensile stress—strain curves of HPDC ACY320 and AM30 alloys at room temperature and 200 °C are shown in Fig. 5. The tensile properties including ultimate tensile strength, tensile yield strength and elongation to failure are listed in Table 1. The strength increases dramatically by 45−65 MPa both at room temperature and 200 °C, while the elongation still keeps a high level with the addition of Ce and Y to AM30 alloy. The following aspects are considered to be related to the improved strength. The first and also the most important aspect is the formation of large amount of $Al_{11}(Ce,Y)_3$ intermetallics which provide considerable reinforcement of dendrite boundaries. Second, since the DAS is finer for the Mg−3Al-based alloys containing Ce and Y, the fine DAS effect can contribute to the observed increase in strength. Another factor is the strengthening of the α-Mg matrix by solid solution with rare earth elements especially Y. Generally, the ductility is low for the alloy containing large amount of intermetallic particles [16]. However, the elongation of HPDC ACY320 alloy with high volume fraction of intermetallics still keeps a high level. It may be related to the fine morphology and arrangement of $Al_{11}(Ce,Y)_3$ intermetallics.

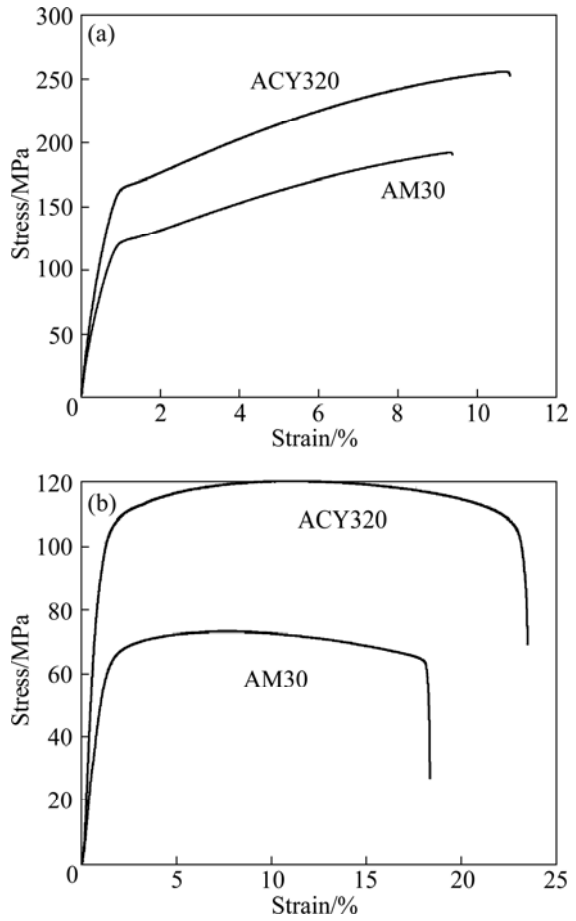

Fig. 5 Typical tensile stress—strain curves of HPDC alloys at room temperature (a) and 200 °C (b)

Table 1 Tensile and compressive properties of HPDC alloys at room temperature and 200 °C

Alloy	Room temperature		
	Tensile yield strength/MPa	Ultimate tensile strength/MPa	Elongation/ %
ACY320	158	255	10
AM30	116	191	9
Alloy	200 °C		
	Tensile yield strength/MPa	Ultimate tensile strength/MPa	Elongation /%
ACY320	103	120	22
AM30	60	72	18

4 Conclusions

1) With the addition of 1.8% Ce and 0.3% Y to Mg−3%Al-based alloy, the primary Mg dendrites are refined, the intermetallic phase $Mg_{17}Al_{12}$ is completely suppressed and substituted by $Al_{11}(Ce,Y)_3$ and $Al_2(Ce,Y)$ with the former being the dominant one at the interdendritic regions.

2) $Al_{11}(Ce,Y)_3$ intermetallics are basically stable at temperature up to 200 °C within 800 h, while most of the $Al_{11}(Ce,Y)_3$ transform to $Al_2(Ce,Y)$ at higher temperature of 450 °C for 800 h. This suggests that the thermal stability of $Al_{11}RE_3$ is conditioned.

3) The high-pressure die-cast Mg−3.0Al−1.8Ce−0.3Y−0.2Mn alloy exhibits significantly improved strength at room temperature and 200 °C, which is the results of the reinforcement of dendrite boundaries with $Al_{11}(Ce,Y)_3$ intermetallics, fine dendritic arm spacing effect as well as the solid solution strengthening with Y element.

References

[1] KULEKEI M K. Magnesium and its alloys applications in automotive industry [J]. Int J Adv Manuf Tech, 2008, 39(9−10): 851−865.

[2] WANG Jian-li, PENG Qiu-ming, WU Yao-min, WANG Li-min. Microstructure and mechanical properties of Mg−6Al−4RE−0.4Mn alloy [J]. Transactions of Nonferrous Metals Society of China, 2006, 16: s1703−s1707.
[3] TONG Guo-dong, LIU Hai-feng, LIU Yao-hui. Effect of rare earth additions on microstructure and mechanical properties of AZ91 magnesium alloys [J]. Transactions of Nonferrous Metals Society of China, 2010, 20: s336−s340.
[4] BAKKE P, WESTENGEN H. Die casting for high performance-focus on alloy development [J]. Adv Eng Mater, 2003, 5(12): 879−885.
[5] ZHU S M, GIBSON M A, NIE J F, EASTON M A, ABBOTT T B. Microstructure analysis of the creep resistance of die-cast Mg−4Al−2RE alloy [J]. Scripta Mater, 2008, 58(6): 477−480.
[6] LUO A A. Recent magnesium alloy development for elevated temperature application [J]. Int Mater Rev, 2004, 49(1): 13−30.
[7] WANG J, LIAO R, WANG L, WU Y, CAO Z, WANG L. Investigations of the properties of Mg−5Al−0.3Mn−*x*Ce (*x*=0−3, wt.%) alloys [J]. J Alloys Compd, 2009, 477(1−2): 341−345.
[8] PETTERSEN G, WESTENGEN H, HØIER R, LOHNE O. Microstructure of a pressure die cast magnesium-4wt.% aluminium alloy modified with rare earth additions [J]. Mater Sci Eng A, 1996, 207(1): 115−120.
[9] HUANG Y D, DIERINGA H, HORT N, MAIER P, KAINER K U, LIU Y L. Evolution of microstructure and hardness of AE42 alloy after heat treatments [J]. J Alloys Compd, 2008, 463(1−2): 238−245.
[10] DARGUSCH M S, ZHU S M, NIE J F, DUNLOP G L. Microstructural analysis of the improved creep resistance of a die-cast magnesium-aluminium-rare earth alloy by strontium additions [J]. Scripta Mater, 2009, 60(2): 116−119.
[11] RZYCHON T, KIELBUS A, CWAJNA J, MIZERA J. Microstructural stability and creep properties of die casting Mg−4Al−4RE magnesium alloy [J]. Mater Charact, 2009, 60(10): 1107−1113.
[12] POWELL B R, REZHETS V, BALOGH M P, WALDO R A. Microstructure and creep behavior in AE42 magnesium die-casting alloy [J]. JOM, 2002, 54(8): 34−38.
[13] ZHANG Jing-huai, YU Peng, LIU Ke, FANG Da-qing, TANG Ding-xiang, MENG Jian. Effect of substituting cerium-rich mischmetal with lanthanum on microstructure and mechanical properties of die-cast Mg−Al−RE alloys [J]. Mater Design, 2009, 30(7): 2372−2378.
[14] ZHANG Jing-huai, LIU H F, SUN W, LU H Y, TANG D X, MENG J. Influence of structure and ionic radius on solubility limit in the Mg−RE systems [J]. Mater Sci Forum, 2007, 561−565: 143−146.
[15] SU Gui-hua, ZHANG Liang, CHENG Li-ren, LIU Yong-bing, CAO Zhan-yi. Microstructure and mechanical properties of Mg−6Al−0.3Mn−*x*Y alloys prepared by casting and hot rolling [J]. Transactions of Nonferrous Metals Society of China, 2010, 20(3): 383−389.
[16] BAE D H, KIM S H, KIM D H, KIM W T. Deformation behavior of Mg−Zn−Y alloys reinforced by icosahedral quasicrystalline particles [J]. Acta Mater, 2002, 50(9): 2343−2356.

Mg−Al−Ce−Y 基压铸合金的微观结构稳定性和力学性能

张景怀[1], 刘淑娟[2], 冷 哲[1], 张密林[1], 孟 健[3], 巫瑞智[1]

1. 哈尔滨工程大学 超轻材料与表面技术教育部重点实验室，哈尔滨 150001；
2. 哈尔滨工业大学 材料科学与工程学院，哈尔滨 150001；
3. 中国科学院 长春应用化学研究所 稀土资源利用国家重点实验室，长春 130022

摘 要：为进一步提高 Mg−Al−RE 基合金的力学性能，采用高压压铸技术制备 Mg−3.0Al−1.8Ce−0.3Y−0.2Mn 合金，并研究其微观组织、金属间相的热稳定性和合金的力学性能。结果表明：合金由细小的初生 α-Mg 枝晶和枝晶间的共晶组成。共晶中存在两种金属间相，即 $Al_{11}(Ce, Y)_3$ 和 $Al_2(Ce, Y)$，其中 $Al_{11}(Ce, Y)_3$ 是主要增强相。研究还表明，$Al_{11}(Ce, Y)_3$ 的热稳定性是有条件限制的，在 200 °C 时效 800 h，它基本保持稳定，而在 450 °C 时效 800 h，绝大部分的 $Al_{11}(Ce, Y)_3$ 发生相分解，转变为 $Al_2(Ce, Y)$。添加 Ce 和 Y 后，合金强度在室温和 200 °C 下得到明显的提高。合金性能的提高主要归因于 $Al_{11}(Ce, Y)_3$ 的形成对枝晶间区域的增强作用、晶粒细化的影响以及由 Y 原子造成的固溶强化。

关键词：镁合金；Mg−Al−Ce−Y 合金；$Al_{11}RE_3$；结构稳定性；力学性能

(Edited by FANG Jing-hua)